

Lunar domes: a generic classification of the dome near Valentine located at 10.26°E and 31.89°N

Raffaello Lena, K. C. Pau, Jim Phillips, Cristian Fattinnanzi & Christian Wöhler

We describe a lunar dome located at longitude 10.26°E and latitude 31.89°N ($\xi = +0.151$ and $\eta = +0.528$), including data about slope and height. An image-based three-dimensional reconstruction of the eastern part of the dome is performed based on shape using a shading approach. This has made it possible to extract additional information for its classification and interpretation in geological terms.

1. Introduction

Lunar domes are formed either by outpouring of magma from a central vent or by a subsurface accumulation of magma that causes an up-doming of the bedrock layers, creating a smooth, gently sloping positive relief.¹

In a prior paper, recently published in the journal of the ALPO,² some of us described a dome, not listed in the ALPO catalogue, located at longitude 10.26°E and latitude 31.89°N ($\xi = +0.151$ and $\eta = +0.528$). The dome, with a dimension of 14×11 km, appears flat and elliptical in shape as a miniature of the famous Valentine dome. The name 'Valentine dome' was coined by Alike Herring for the well known dome at longitude 10.18°E and latitude 30.66°N.³

This elusive dome was added to the unpublished revised lunar dome catalogue by Robert A. Garfinkle, FRAS and to the unpublished revised list by Charles Kapral.⁴

In this study we report further measurements and include new CCD imaging of the lunar dome located at 10.26°E and 31.89°N. This has made it possible to extract additional information (slope and height) for its classification and interpretation.

2. Instruments and measurements

Table 1 lists the 13 observers who supplied a total of 29 observations. This report is based on an analysis of 8 visual observations and 21 images taken under different solar altitude (Table 3). We strongly encouraged observers to participate in organised, simultaneous observations. Such effort significantly reinforced the level of confidence that we have in our data. The images and the shadow analysis were consistent and, in some cases, the images were obtained in contemporaneous and independent sessions.

For each of the observations, the local lunar altitude of the Sun (Alt), the azimuth of the Sun (Az), and the Sun's

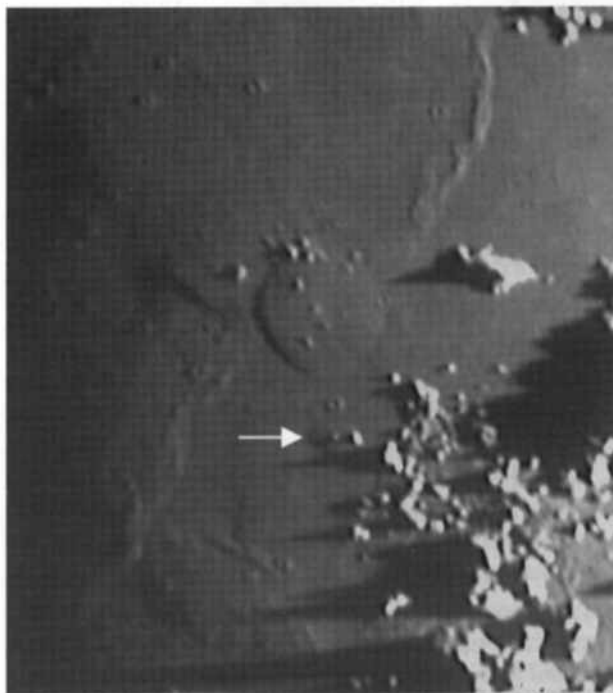


Figure 1. Image by Phillips on 2004 August 7 at 10:23 UT (Alt=1.98°, Col=168.36°, Az=270.57°; seeing II Antoniadi scale). 203mm f/9 refractor. South is up and west (IAU) to the right in all images.

selenographic colongitude (Col) were calculated using the *Lunar Observer's Toolkit* by H. D. Jamieson (ALPO).⁵ Table 2 reports the position of the dome and the coordinates of the hill that lies on its north-west (IAU) flank. The coordinates were obtained by superimposing our images onto Rukl's map (chart #13). Furthermore, we were able to distinguish between the black shadow and the dark grey shading (penumbra) of the dome's flank which represents grazing illumination by sunlight. On the best images, the dome diameter and the length of its shadow were both measured in pixels. The corresponding scale of the image was obtained, allowing diameters and shadow lengths to be expressed in kilometres. The measured heights were also calculated using the *Lunar Observer's Toolkit* software. The results are summarised in Table 4.

3. Vertical cross-section of the dome

Information about the vertical cross-section was obtained using three methods, as follows:

a) Maximum slope

The dome located at 10.26°E, 31.89°N has a flat summit with low height. The flank steepness 's' is equal to the solar height when the black shadow cast by the flank appears (in sunset) or disappears (in sunrise). It corresponds to the maximum slope angle. The average east flank width 'w' can be estimated using high resolution images (Table 4).

The height (H) of the dome can be then calculated by the formula:

$$H = w \times (\tan s) \quad [1]$$

b) Effect of the slope, Hill height method

The height of the dome was also estimated by comparing the shadow lengths of the hill that lies on the northwest flank of the dome (Table 2).

This hill, under evening illumination, casts a shadow on the dome summit while under morning illumination it casts a shadow to the lunar surface.

Obviously the shadow length measured under evening illumination will be shorter (upward slope). It is expected that the hill, under morning illumination, has a larger height value (h_m) because the



Figure 2. Image by Pau on 2003 October 16 at 21:02 UT (Alt=3.44°, Col=166.15°, Az=268.74°; seeing II Antoniadi scale). 250mm f/6 Newtonian.

Table 1. Contributing observers and instruments

Observer	Instrument	Type	No. of reports
			M=Morn. illum. E=Evening illum.
Cicognani M.	410mm Cassegrain f/17	Visual, CCD	4M
Chu A.	250mm Newtonian f/6	CCD	1E
Cocco A.	200mm SCT f/10	CCD	1E
Crandall E.	250mm Newtonian f/6	CCD	1M
Fattinanzi C.	250mm Newtonian f/5	CCD	1E
Lena R.	100mm refractor f/15	Visual, digital camera	2M, 3E
Nardella S.	180mm Maksutov f/6	CCD	1M
Pau K. C.	250mm Newtonian f/6	CCD	2M, 2E
Phillips J.	203mm refractor f/9	CCD	2M, 1E
Sforza A.	200mm SCT f/10	CCD	1E
Shaw B.	125mm refractor f/8 250mm Newtonian f/12	CCD	4E, 1M
Vignale G.	200mm SCT f/10	CCD	1E
Villares F.	200mm SCT f/10	Digital camera	1M

shadow tip is not on the dome summit but on the lunar surface to the northwest. Using this method we were able to obtain two different height values under morning illumination (h_m)

and evening illumination (h_e) respectively. The height (H) of the dome was then calculated by the formula:

$$H = h_m - h_e \quad [2]$$

The results are summarised in Tables 5 and 6.

c) Image-based 3D reconstruction of the dome

A well-known method for 3D surface reconstruction is shape-from-shading. It makes use of the fact that surface parts inclined towards the light source appear brighter than surface parts inclined away from it. Traditional applications of this technique in planetary science, mostly referred to as photoclinometry, are designed to reveal a set of profiles along one-dimensional lines.⁹ Techniques for 3D reconstruction of complete surfaces have been developed in the field of computer vision,⁷ also dealing with the combination of shading and shadow features.⁸ The shape-from-shading approach described in Ref. 7, which will be used in this paper, aims at deriving the slope of the surface in east-west and north-south directions together with a consistent height value z for each image pixel, based on the pixel intensities of the image.

To determine a shape using shading analysis, the reflectance properties of the surface, describing how it interacts with incident light, must be known. A simple example is a diffusely scattering or Lambertian surface. In this case, the intensity I_{model} of reflected light obeys the Lambert law $I_{\text{model}} = \rho \cos \theta$ with θ as the angle between surface normal and direction of incident light and ρ as the so-called surface albedo, which is assumed to be constant. For oblique illumination as in Figures 1–5, we have values of θ slightly less than 90°. The reflectance behaviour of the lunar surface somewhat differs from the Lambertian model. It can be described by the Lunar-Lambert law which not only shows a dependence of I_{model} on $\cos \theta$ but also on the angle under which the surface is observed.

Table 2. Position of the dome near Valentine and of the hill that lies on its northwest flank

Feature	Position (Lunar orthographic coordinate)		Position (Longitude, Latitude)	
	ξ	η	(°)	(°)
Dome	+0.151	+0.528	+10.26	+31.89
Hill	+0.147	+0.529	+ 9.95	+31.91

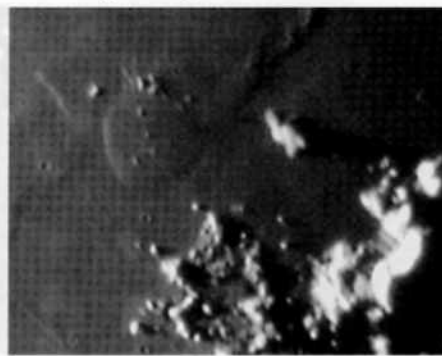


Figure 3. Image by Pau on 2004 December 30 at 11:51 UT (Alt=3.32°, Col=354.39°, Az=93.48°; seeing II Antoniadi scale).

The height (H) of the dome was then calculated by the formula:

$$H = h_m - h_e \quad [2]$$

The results are summarised in Tables 5 and 6.

c) Image-based 3D reconstruction of the dome

A well-known method for 3D surface reconstruction is shape-from-shading. It makes use of the fact that surface parts inclined towards the light source appear brighter than surface parts inclined away from it. Traditional applications of this technique in planetary science, mostly referred to as photoclinometry, are designed to reveal a set of profiles along one-dimensional lines.⁹ Techniques for 3D reconstruction of complete surfaces have been developed in the field of computer vision,⁷ also dealing with the combination of shading and shadow features.⁸ The shape-from-shading approach described in Ref. 7, which will be used in this paper, aims at deriving the slope of the surface in east-west and north-south directions together with a consistent height value z for each image pixel, based on the pixel intensities of the image.

To determine a shape using shading analysis, the reflectance properties of the surface, describing how it interacts with incident light, must be known. A simple example is a diffusely scattering or Lambertian surface. In this case, the intensity I_{model} of reflected light obeys the Lambert law $I_{\text{model}} = \rho \cos \theta$ with θ as the angle between surface normal and direction of incident light and ρ as the so-called surface albedo, which is assumed to be constant. For oblique illumination as in Figures 1–5, we have values of θ slightly less than 90°. The reflectance behaviour of the lunar surface somewhat differs from the Lambertian model. It can be described by the Lunar-Lambert law which not only shows a dependence of I_{model} on $\cos \theta$ but also on the angle under which the surface is observed.

Table 2. Position of the dome near Valentine and of the hill that lies on its northwest flank

Feature	Position (Lunar orthographic coordinate)		Position (Longitude, Latitude)	
	ξ	η	(°)	(°)
Dome	+0.151	+0.528	+10.26	+31.89
Hill	+0.147	+0.529	+ 9.95	+31.91

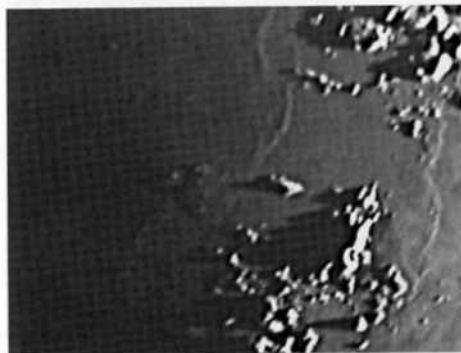


Figure 4. Image by Fattinanzi on 2004 September 5 at 23:10 UT (Alt=1.23°, Col=169.01°, Az=270.63°; seeing II–III Antoniadi scale). 250mm f/5 Newtonian.

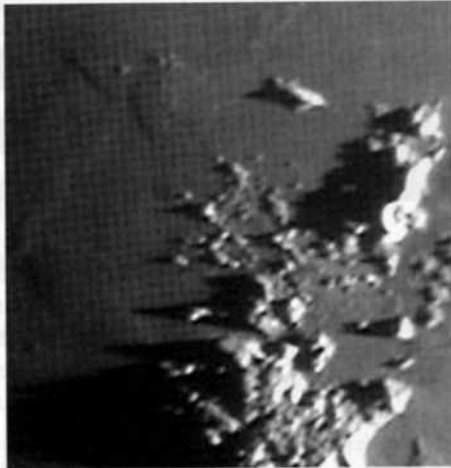


Figure 5. Image by Pau on 2003 February 22 at 19:58 UT (Alt=2.97°, Col=165.29°, Az=266.36°; seeing II–III Antoniadi scale).

The shape-from-shading algorithm adjusts for each pixel position (x,y) the slope of the model surface such that the resulting average deviation $\langle [I_{\text{obs}}(x,y) - I_{\text{model}}(x,y)]^2 \rangle$ between observed and modelled intensity of reflected light is minimised. The height profile $z(x,y)$ is obtained by integration of the surface slopes. In section 5.1 of Ref. 7, an iterative formula is derived for the surface slopes in east–west and north–south directions and the height z of each pixel. It is straightforward to implement this iteration as a computer program. The iterative scheme consists of the following steps:

1. Set $z(x,y) = 0$ as the initial height for each pixel. Consequently, the initial surface slopes are zero as well.
2. Compute the albedo ρ based on the current values of the surface slopes.

Table 3. Observations of the dome located at 10.26°E, 31.89°N under morning and evening illumination

Remarks describe the aspect of the umbra or penumbra cast by the partly illuminated dome's flank.

Date and time (UT)	Illumination		Type	Remarks
	M=Morning E=Evening	Solar altitude		
2004 Jan 28, 19:37	M	0.17°	CCD	Shadow entered the terminator
2003 Nov 30, 13:12	M	0.18°	CCD	Shadow entered the terminator
2004 Jan 28, 19:40	M	0.19°	CCD	Shadow entered the terminator
2004 May 25, 20:30	M	0.20°	visual	Shadow entered the terminator
2004 Jan 28, 19:50	M	0.27°	visual	Shadow entered the terminator
2004 May 25, 20:56	M	0.31°	visual	Shadow entered the terminator
2004 May 25, 21:15	M	0.40°	visual	Shadow entered the terminator
2004 Mar 27, 23:15	M	0.51°	visual	West foot dark
2004 Jul 23, 19:19	M	0.95°	CCD	Slight umbra with west foot dark
2004 Jul 23, 19:35	M	1.07°	visual	Slight umbra with west foot dark
2004 Nov 3, 22:58	E	1.19°	CCD	Dark shadow (umbra)
2004 Sep 5, 23:10	E	1.23°	CCD	Dark shadow (umbra)
2004 Sep 5, 23:20	E	1.24°	visual	Dark shadow (umbra)
2003 Oct 17, 01:33	E	1.52°	CCD	Dark shadow (umbra)
2004 Aug 7, 10:15	E	1.98°	CCD	First trace of dark shadow (umbra)
2003 Nov 30, 17:35	M	2.06°	visual	Penumbra
2003 Apr 8, 18:28	M	2.15°	CCD	Penumbra
2003 Nov 30, 18:00	M	2.24°	visual	Penumbra & photo
2004 Sep 5, 20:46	E	2.28°	CCD	Penumbra
2004 Jan 29, 00:33	M	2.29°	CCD	Penumbra
2003 Feb 22, 19:58	E	2.96°	CCD	Penumbra
2003 Dec 30, 11:51	M	3.32°	CCD	Penumbra
2003 Oct 16, 21:02	E	3.44°	CCD	Penumbra
2004 Aug 7, 01:45	E	5.71°	CCD	–
2003 Sep 17, 00:36	E	7.15°	CCD	–
2004 Nov 3, 01:50	E	10.26°	CCD	–

3. For each pixel (x,y) , update the surface slopes by a small amount such that $\langle [I_{\text{obs}}(x,y) - I_{\text{model}}(x,y)]^2 \rangle$ is reduced.

4. Update the height $z(x,y)$ according to the new slope values.

5. Repeat steps 2–4 until the average deviation $\langle [I_{\text{obs}}(x,y) - I_{\text{model}}(x,y)]^2 \rangle$ does not decrease any more.

After this computation, a height level z is available for each pixel. In this framework, the level of zero height $z = 0$ is set arbitrarily. The effective height of a dome is then given by the difference between the $z(x,y)$ values on its summit and the surrounding surface, respectively.

Only the eastern flank of the dome north of Valentine was reconstructed because the reconstruction of its western part is affected by the shadows cast across its surface by the protrusions on its centre and western flank. These shadows lead to strong distortions of the reconstructed surface profile.

To obtain an accurate 3D reconstruction result by means of shape-from-shading algorithms, it is necessary that the grey value G of a pixel is proportional to the intensity I of incident light. For many CCD cameras and especially webcams, this is not necessarily the case because it is often possible to adjust the gamma value manually from within the camera control software,

such that the relation between grey value and intensity is governed by $G \sim I^\gamma$. For the images used for 3D reconstruction, no actual gamma calibration was performed, but the camera control parameters used during image acquisition imply that one may assume that γ lies in the interval 0.8 ... 1.2. We have shown experimentally that this uncertainty about the value of γ results in about 20% relative error of the computed surface gradients and therefore the effective height of the dome. The results presented in Section 5, however, are in good accordance with height measurements obtained by shadow analysis (see above), such that the value of γ probably does not differ significantly from 1 for the images used for 3D reconstruction.

4. Observations

We received 15 observations from 9 observers for evening illumination and 14 observations from 8 observers for morning illumination (Table 1). Examples of images are shown in Figures 1–5, all oriented with south upwards, and west (IAU) on the right. Seeing is reported using the Antoniadi Scale.

Table 4. Height of the dome measured on Figure 1

Data	Illum.	Solar altitude	Flank width w (pixels)	Flank width w (km)	Measured height (m)
Fig. 1	E	1.98°	5 ± 1	2.04±0.41	71 ± 14

using a 100mm refractor at $f/15$. The drawing is given as Figure 6. Two additional drawings by Massimo Cicognani and Lena are given in Figures 9 and 10.

5. Results and discussion

This dome requires a specific solar altitude to be observed clearly and a narrow solar angle for maximum detail. A penumbra (not black shadow) is visible from $H = 2.1^\circ$ to $H = 4.0^\circ$ and certainly up to $H = 7.0^\circ$ (Table 3). In Figure 1, made at solar altitude of 1.98° , the first black shadow (umbra) was detected under evening illumination. In Figures 2 and 3, made at solar altitude values $>2.0^\circ$, the dome does not cast a black shadow but only a penumbra on the partly illuminated flank. From Tables 2 and 3, it follows that the maximum slope angle of the dome is about 1.98° . The height of the dome was then estimated using Formula 1 and the *Lunar Observer's Toolkit* software. It turns out that the summit of the dome is 71 metres higher than the surrounding plain.

This estimated height is comparable with the values measured using the method described in Section 2b (Tables 5–6). Using this method we calculated a height of 76 metres. These measurements provide some insight into a possible explanation for the small height variations. The dome is very flat and the shadow cannot be cast from the top of the dome but only from a point of its steeper flanks.

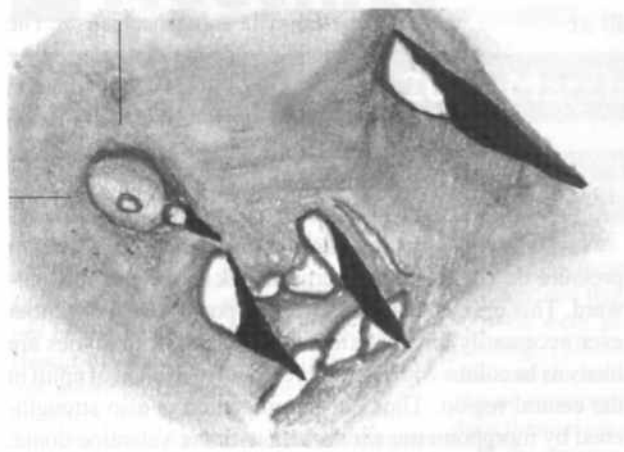


Figure 6. Drawing by Lena, 2003 November 30 at 17:35 UT (Alt=2.06°, Col=352.49°, Az=91.88°; seeing II Antoniadi scale). 100mm refractor at $f/15$.

Figure 1 displays the dome under an evening illumination. This image was taken by Phillips using a 203mm $f/9$ refractor on 2004 August 7 at 10:23 UT.

Figure 2 was taken by Pau on 2003 October 16 at 21:02 UT using a 250mm $f/6$ Newtonian.

A further image (Figure 3) was obtained under morning illumination by Pau on 2004 December 30 at 11:51 UT.

Figure 4 displays the dome under a lower solar altitude. This image was taken by Fattinnanzi using a 250mm $f/5$ Newtonian during an observation carried out on 2004 September 5 at 23:10 UT. This is one of the many images obtained under a lower solar altitude. In this frame (evening illumination), the dome's east foot still shows a black shadow fused with the shadows of nearby isolated peaks.

Another image (Figure 5) was made by Pau on 2003 February 22 at 19:58 UT, under evening illumination. The dome's eastern flank does not show a shadow on this image, but its gentle slope is nevertheless apparent. Lena made an observation of this region on 2003 November 30 at 17:35 UT

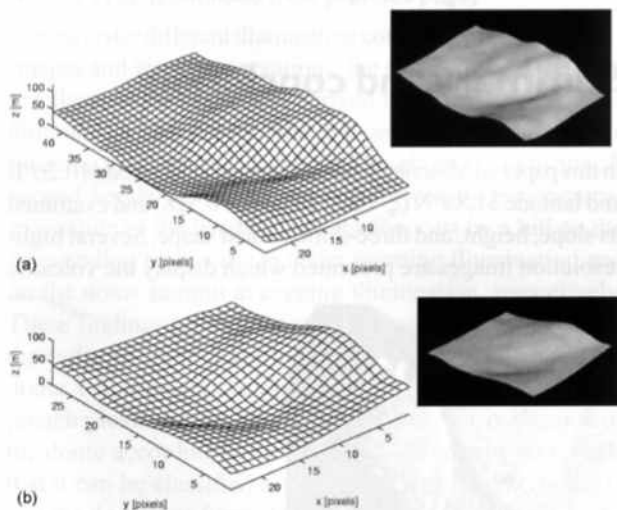


Figure 7. 3D reconstruction results obtained by means of the shape-from-shading method described in the text. Figures 7a and 7b both display the eastern flank of the dome, derived from Figures 2 and 5, respectively. The mesh representations (left column) illustrate the measured height quantities, while the rendered views (right column, height exaggeration by a factor of 20) attempt to give a realistic 3D impression of the dome. All scenes are viewed from the northeast.

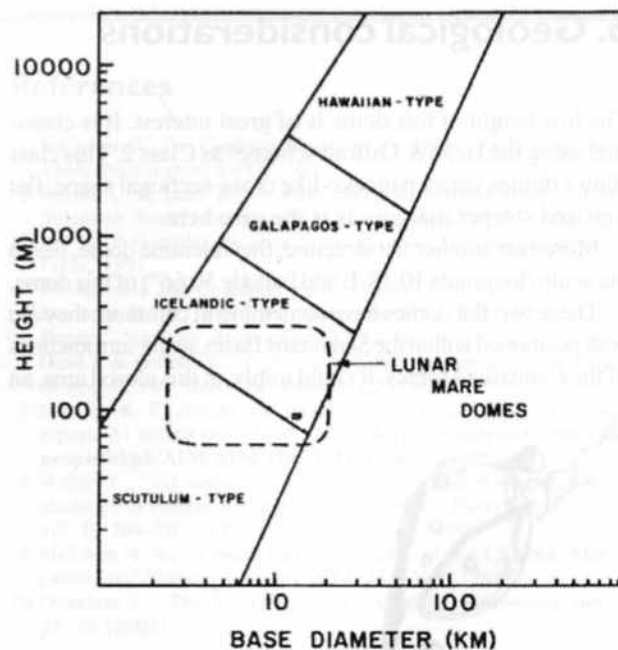


Figure 8. Morphometry. As described in the text, an intrusive origin for several flat domes cannot be established or ruled out on the basis of the diagram published in Ref.6. (James W. Head & Ann Gifford)

Table 5. Measurement of the shadow lengths of the hill at 9.95°E, 31.91°N

Data	Illum.	Solar altitude	Shadow length		Measured height (m)	Remarks
			(pixel)	(km)		
Fig. 2	E	3.71°	11±1	3.85±0.35	260±28	shadow tip on dome summit
Fig. 3	M	3.05°	21±1	6.30±0.30	336±16	shadow tip on soil

Table 6. Height of the dome located at 10.26°E and 31.89°N obtained using the hill height method

Evening illumination Hill height	Morning illumination Hill height	Dome height
260m	336m	76m

Figure 7 shows the 3D reconstruction results obtained by means of the shape-from-shading method described in detail in section 5.1 of Ref. 7. Figures 7a and 7b both display the eastern flank of the dome, derived from Figures 2 and 5, respectively. The mesh representations (left column) illustrate the measured height quantities, while the rendered views (right column, height exaggeration by a factor of 20) attempt to give a realistic 3D impression of the dome. All scenes are viewed from the northeast. The effective height of the dome measured from the 3D profiles in Figure 7 amounts to 80 ± 16 m. A height of 80 m was also measured by means of a reconstruction of the northern flank of the dome based on Figure 1 (profile not shown here). As pointed out in Section 3c, the relative accuracy of these height values is estimated to 20%. They are, however, in good correspondence with the height values in Table 4 and Table 6 obtained by shadow analysis.

6. Geological considerations

The low height of this dome is of great interest. It is classified using the Head & Gifford scheme⁶ as Class 2. This class shows domes with a pancake-like cross-sectional shape, flat tops and steeper margins as is the case here.

Moreover another flat structure, the Valentine dome, lies to the south (longitude 10.18°E and latitude 30.66°) of this dome.

These two flat domes have something in common: they are both positioned within the Serenitatis Basin, in the surroundings of the Caucasus Montes. It could imply, in this closed area, an



Figure 9. Drawing by Massimo Cicognani, 2004 May 25 at 20:30 UT. Seeing II Antoniadi scale. 410mm Cassegrain at f/17.

origin based on the same mechanism. The tops of both domes are flat suggesting that there was not a gradual inclination at the vent (the rising lava did not build up the dome in a series of flows) but a subsurface intrusion of magma.

In this scenario rising lavas accumulate within the lunar crust increasing in pressure slowly, causing the crustal rock above it to bow outward. This creates a structure of low positive relief without ever necessarily having external eruptions. Both domes are likely as laccoliths with lateral spread and relaxation of uplift in the central region. Thus our interpretation is also strengthened by morphometric similarities with the Valentine dome, such as presence of peaks on its surface and albedo similarities, as recently published in Refs. 2 & 10. Further, most lunar domes that are hemispherical and have pits are formed by outpouring of magma from a central vent (effusive eruptions). The extrusive origin of lunar domes and their similarity to terrestrial features, as small shield volcanoes, has been described in Ref. 6.

As a note of interest, the height–base diameter relationship for the examined dome (see Figure 8) matches the terrestrial example of the Icelandic type in the diagram published in Ref. 6. But the fact that the morphometry of the dome (measurements and dimensions) is consistent with Icelandic shields does not prove that this dome is a shield. An intrusive origin for several flat domes (as is the case here) cannot be established or ruled out on the basis of the diagram published in Ref. 6. Numerous authors have reported similarities of many effusive lunar domes to terrestrial volcanic features, but additional work is necessary for intrusive lunar domes to be compared with apparent equivalent features on the Earth. Variations between terrestrial and lunar structures make the comparison uncertain without additional studies on the mechanisms of intrusions under lunar conditions.

Summary and conclusion

In this paper we described a dome located at longitude 10.26°E and latitude 31.89°N ($\xi +0.151$ and $\eta +0.528$) and examined its slope, height, and three-dimensional shape. Several high-resolution images are presented which display the volcanic

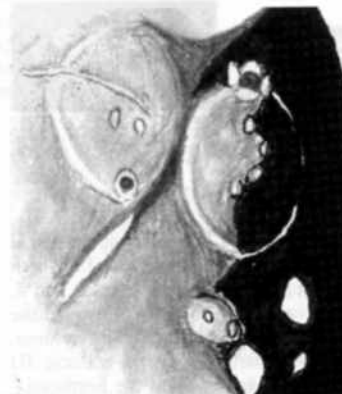


Figure 10. Drawing by Lena, 2004 January 28 at 19:50 UT. Seeing II Antoniadi scale. 100mm refractor at f/15. The dome is emerging from the shadows.

Ordinary Meeting, 2005 March 30

held at The Geological Society, Burlington House, Piccadilly, London W1

Tom Boles, President
Ron Johnson and Nick Hewitt,
Secretaries

Mr Boles opened the fifth Ordinary Meeting of the 115th session, and invited Dr Hewitt to read the minutes of the previous meeting. These met the approval of members, and were duly signed. Mr Ron Johnson, Business Secretary, reported that three books had been received: *Mary Somerville*, by Dr Allan Chapman, and Sir Patrick Moore's autobiography, both donated by Mr A. J. Kinder, and *Big Ben, The Bell, The Clock*, by Peter MacDonald,

donated by its author. Members applauded the donors. The President reported that fifteen new members were proposed for election, and that Council had elected the 49 who were proposed at the previous meeting. This being accepted, they were declared elected, and the President invited any newcomers in the audience to introduce themselves to him after the meeting.

In the absence of the Papers Secretary, Mrs Hazel McGee announced the approval of five papers for *Journal* publication:

Predicting astronomical seeing in the UK,
by Damian Peach

The 2004 transit of Venus observed from the Open University observatory, by Peter Chambers *et al.*

The discovery of the correct birth date for selenographer Thomas Gwyn Empey Elger, by Robert Garfinkle

The 'Sky at Night' goes south, by Damian Peach

Lunar domes: a generic classification of the dome near Valentine located at 10.26°E and 31.89°N, by Raffaello Lena *et al.*

The President said that the next Ordinary Meeting would be held at 14:30 on Saturday April 23, when the main speaker would be Dr Omar Almaini of the University of Nottingham, speaking on *Quasars, Black Holes and Galaxy Formation*. In other news, he extended his warmest congratulations to Guy Hurst, a former BAA President, who had received the Royal Astronomical Society's 2005 Award for Services to Astronomy in recognition of his work within the amateur astronomical community, both administrative and observational. Mr Hurst's work in forging and strengthening Pro-Am collaborations had received particular commendation.

Moving onto administrative matters, Mr Boles reported with regret that Ms Anne Davies had departed the office, and a presentation was made in recognition of her services to the Association. He was pleased to announce that on March 23, a new Office Manager, Ms Jean Felles, would be starting work.

Special General Meeting, 2005 March 30

held at The Geological Society, Burlington House, Piccadilly, London W1

Tom Boles, President
Ron Johnson and Nick Hewitt,
Secretaries

The President opened the Special General Meeting of the 115th session, inviting Dr Hewitt to read the minutes of the previous year's SGM, which were approved by the members.

Mr David Tucker, Treasurer, was asked to comment on the Association's finances. He said that Council proposed an increase

of two pounds in the standard subscription rate for the 116th session, accompanied by a pro-rata increase in the reduced rates. Mr Tucker invited questions concerning this, and there being none, proposed its adoption. The motion was seconded, and passed by the members.

Mr Boles adjourned the meeting until 2006 March, and the fifth Ordinary Meeting of the session followed.

Dominic Ford

► Lena *et al.* (continued from previous page)

feature under different illumination conditions. Based on CCD images and visual observations, the slope angle of the eastern flank of the dome was derived by estimating the solar altitude at which the first shadow cast by the dome appears (evening illumination), leading to a height of 71 ± 14 metres. A second height value of 76m was derived by bidirectional evaluation of the length of the shadow cast by a hill on the surrounding mare surface under morning illumination and on the dome summit at evening illumination, respectively. These findings are supported by the results of image-based three-dimensional reconstruction of the eastern flank of the dome, employing a shape-from-shading technique. This approach yields a dome height of 80 ± 16 m. A classification of the dome according to the Head & Gifford scheme reveals that it can be classified as of Class 2. Our interpretation is that the dome was formed by rising lava collecting in a sub-surface pocket, most likely a laccolith.

Address (RL): Geologic Lunar Research Group [GLR] Coordinator,
Via Cartesio 144, 00137 Rome, Italy. [lena@glrgroup.org]

References

- 1 Wilhelms D., *The Geologic History of the Moon*, USGS Prof. Paper 1348, Washington: GPO, 1987
- 2 Pau K. C. & Lena R., 'A study about an unlisted dome near the Valentine dome', *Strolling Astronomer*, **46**(4), 25–27 (2004)
- 3 Hill H., *A Portfolio of Lunar Drawings*, p.16, Cambridge University Press, 1991
- 4 B. Garfinkle and C. Kapral, *pers. comms.*, 2004
- 5 Jamieson H. D., 'The Lunar Dome Survey – Fall 1992 Progress Report', *Strolling Astronomer*, **37**(1), 14–17 (1993)
- 6 Head J. & Gifford A., 'Lunar mare domes: classification and modes of origin', *The Moon and Planets*, **22** (1980)
- 7 Horn B. K. P., *Height and Gradient from Shading*, MIT technical report, AI memo no. 1105A, 1989, <http://people.csail.mit.edu/people/bkph/AIM/AIM-1105A-TEX.pdf>
- 8 Wöhler C., '3D surface reconstruction by self-consistent fusion of shading and shadow features', in *Int. Conf. on Pattern Recognition*, vol. II, 204–207, IEEE Computer Society, 2004
- 9 McEwen A. S., 'Albedo and Topography of Ius Chasma, Mars', *Lunar and Planetary Science XVI*, 528–529 (1985)
- 10 Douglass E., 'The Valentine dome', *Strolling Astronomer*, **46**(1), 21–23 (2004)

Received 2004 December 21; accepted 2005 March 30